The Effect of Deep Defects on the Efficiency Variation of $CH_3NH_3PbI_3$ Perovskite Solar Cells

Nipuna L Adihetty
Faculty of Graduate Studies
University of Sri Jayewardenepura
Nugegoda, Sri Lanka
nladhi@sjp.ac.lk

Dinuka R Ratnasinghe
Faculty of Graduate Studies
University of Sri Jayewardenepura
Nugegoda, Sri Lanka
dinuka@sjp.ac.lk

Muthuthanthrige L. C. Attygalle
Department of Physics
University of Sri Jayewardenepura
Nugegoda, Sri Lanka
lattygalle@sci.sjp.ac.lk

Som Narayan
Department of Physics
The Maharaja Sayajirao University of Baroda
Gujarat, India
somnarayan4@gmail.com

Prafulla K Jha
Department of Physics
The Maharaja Sayajirao University of Baroda
Gujarat, India
prafullaj@yahoo.com

2021 Moratuwa Engineering Research Conference (MERCon) | 978-1-6654-3753-0/21/$31.00 ©2021 IEEE | DOI: 10.1109/MERCON52712.2021.9525651

***Abstract*— Three-dimensional (3D) halide perovskites as $CH_3NH_3PbI_3$ (3D-MAPI) have shown high performance in the perovskite solar cells. However, deep defects due to lattice disorders in the 3D halide perovskite cause to limit the performance of the halide perovskite solar cells. We have numerically simulated and investigated the optimum deep defect density of the 3D-MAPI layer of the p-i-n solar cell model with the structure of Glass/ITO(TCO)/PEDOT: PSS(HTM)/i-2D-MAPI/i-3D-MAPI/i-2D-MAPI/PCBM(ETM)/Ag. Due to the degradation of the organic components under some environmental conditions, the Pb-based organic perovskite solar cells need protective films. This 2D-3D-2D perovskite solar cell has been modeled as a stable perovskite solar cell, by inserting thin 2D-MAPI layers on both sides of the 3D-MAPI to reduce the degradation and moisture issues. Using SCAPS-1D solar cell simulation software, the deep defect density in the 3D halide perovskite layer was optimized to obtain the best performance of the cell model. Our simulation results have indicated that the deep defect density of the 3D-MAPI layer should not exceed 10^{12} cm^{-3} for high performance. Also, low dark saturation current density and low Shockley-Read-Hall (SRH) recombination current density were observed at the low deep defect density in the 3D-MAPI layer.**

Keywords—perovskite solar cell, protective-layer, dark saturation current, deep defects, power-conversion efficiency

I. INTRODUCTION

The global energy requirement has increased due to the development of technology and the increment of electricity usage [1]. Therefore, the developments of renewable energy sources as solar energy have acquired more attention. The low cost and higher efficiency renewable energy sources are popular all over the world. The generation of electricity by using solar cells has received more attention due to the rapid developments of solar cell technologies and the increment of solar cell efficiency. There are many Photovoltaic (PV) technologies. Among them, Perovskite-based solar cell technology has become promising technology due to the rapid development of efficiency and low production cost.

Organic-Inorganic Halide perovskites are emerging materials in solar cell production due to their extraordinary material properties, which are tunable optical bandgap, weak exciton binding energy, and good absorption property. These special material properties of the halide perovskites cause to show high performances. Halide perovskites also show low material cost, low processing cost, and higher power conversion efficiencies. According to the efficiency chart of the National Renewable Energy Laboratory [2], the power conversion efficiency of the single-junction perovskite-based solar cell has acquired 25.2%. Halide perovskite can be represented by using a general formula as ABX_3, where A is an organic cation as $CH_3NH_3^+$, B is an Inorganic cation as Pb^{2+}, and X is a halogen ion as I^- [3]. Methylammonium lead iodide ($CH_3NH_3PbI_3$), which is also called 3D-MAPI, is one of the most popular halide perovskites in the solar cell industry since it shows good performance and low production cost. However, Methylammonium lead iodide is considered as one of the three-dimensional (3D) perovskite materials, which are unstable with moisture and oxygen. Therefore, 3D-perovskite-based solar cells can degrade after long-term exposure to the external surrounding. Consequently, 3D-perovskite-based solar cells have shown low light-absorbing ability and performance in the external surrounding [4]. Moreover, two-dimensional (2D) Ruddlesden-Popper halide perovskites are used to increase the stability of three-dimensional (3D) halide perovskite since 2D Ruddlesden-Popper halide perovskites act as a moisture blocking layer, which can increase the resistance for the moisture [5]. The combination of 2D and 3D halide perovskite layers have acquired more attention in the perovskite solar cells due to their moisture stability and good performance [5-7]. In this simulation study, we have numerically tried to develop and predict an efficient solar cell device model with low degradation by sandwiching the 3D-MAPI between two 2D-MAPI layers since 2D-MAPI can increase the stability of the solar cell by reducing the degradation issue of 3D-MAPI. The perfect photo-conversion process is limited due to the carrier recombination occur by the defects in solar cell materials. The main recombination processes that occur in a semiconductor material can be listed as Radiative, Auger, and Shockley-Read-Hall (SRH), recombination [8]. Radiative recombination occurs when an electron that comes from a conduction band recombines with a hole that is in the valence band. In this Radiative Recombination process, photons are emitted. Auger recombination is another recombination process in which an electron that is in the conduction band and hole that is in the valence band recombine and emit the energy. Then, the emitted energy is transferred to another electron that is in the conduction band, which is excited by the emitted energy. Auger recombination mainly occur at higher charge carrier concentrations of the heavily doped materials or high injection of carriers under concentrated photon condition. Lattice

Ministry of Science, Technology and Research, Government of Sri Lanka.

978-1-6654-3753-0/21/$31.00 ©2021 IEEE

defects do not encourage Radiative recombination and Auger recombination in the 3D bulk MAPI [9, 10]. Point defects that are lattice defects cause to occur SRH recombination. Shallow and deep defects are created by point defects in the semiconductor. Among them, deep defects mainly limit the performance of the material. 3D-MAPI also faces this phenomenon [9], since deep defects mainly control the performance of the 3D-MAPI. According to that, high deep defect density causes the reduction of the performance in 3D-MAPI. Also, SRH recombination in 3D-MAPI can be reduced by controlling the deep defect density. The effect of the deep defects, which are in the 3D-MAPI layer, were studied by altering the deep defect density in 3D-MAPI. This modeling study will be useful to get an idea about the impact of the deep defect density in the 3D-MAPI layer of the cell model. This numerical model can lead the future experimental approaches towards a best perovskite-based p-i-n type solar cell. We have fit the best numerical model by optimizing the solar cell performances according to the deep defect concentrations introduced in 3D-MAPI.

II. Methodology

Fig. 1 illustrates the baseline cell structure that was developed in the numerical modeling study of the previous work [11]. In this approach, we have selected 2D-MAPI as a very thin protective film (~0.1 ($3D\text{-}MAPI_{length}$)), instead of a thick layer introduced in the baseline model 1 [11]. In this cell structure, Indium-tin oxide (ITO), which is a transparent conducting oxide (TCO) that is an optically transparent electrode, has been selected as a front contact material by calculating the work function of the front contact [12, 13]. PEDOT:PSS (poly(3,4-ethylenedioxythiophene):poly(4-styrenesulfonate)) is a conductive polymer, which is p-type hole acceptor material in which the majority-carriers are holes. The cell performance has been enhanced by adding an intrinsic absorber, which is Methylammonium lead iodide (3D-MAPI). Intrinsic Two dimensional (2D)-sheets of Methylammonium lead iodide (2D-MAPI) were used as protective layers for 3D-MAPI (Bandgap = 1.55 eV). This solar cell model consists of the 3D-MAPI layer sandwiched between two thin 2D-MAPI (Bandgap = 1.63 eV) layers, which were introduced to increase the stability of the solar cell [5]. Shallow and deep defects have been introduced in the 3D-MAPI ($CH_3NH_3PbI_3$) layer in the solar cell model. Shockley-Read-Hall (SRH) recombination are occurring through the deep and shallow defect states that act as SRH recombination centers, which are created by deep and shallow defects in the 3D-MAPI layer. Also, Auger and Radiative recombination are slightly occurring in the 3D-MAPI layer. But the effect of Radiative and Auger recombination was considerably low since the heavily doped condition and concentrated photon condition were not used in this simulation study. The radiative recombination effect is not so important in this simulation since the carrier concentration in the 3D-MAPI layer is 10^{16} cm^{-3}, which is not considered as a heavily doped condition. Radiative recombination is mainly determined at high carrier injection levels. In this simulation study, Auger recombination cannot give a considerable impact on the results. Auger recombination is considerably low under the condition of one sun illumination (AM1.5G spectrum), which is not a concentrated photon condition [9]. Any defects have not been included in the 2D-MAPI layer since it has shown very low point and interfacial defect density [14]. Also, any carrier recombination effect of the 2D-MAPI layer was not included in this simulation study. In this solar cell model, PCBM ((6, 6)-phenyl-C61-butyric acid methyl ester) is used as an n-type layer in which the majority carriers are electrons. The back contact material has been selected by calculating the work function of the back contact, which is close to the work function of Silver [15] in this cell model. The baseline cell model was numerically developed by using the material parameters, which were extracted from the previous experimental and theoretical studies [16-21].

The 2D/3D/2D baseline cell model was numerically simulated by using SCAPS-1D simulation software. Here the changes in the cell performance were observed by changing the deep defect density concentrations in the 3D-MAPI layer. Deep defect density in 3D-MAPI has been experimentally identified with the range of 10^{14}-10^{16} cm^{-3} in the previous studies [15, 22]. However, the deep defect density in the 3D-MAPI layer was varied from 10^{10} to 10^{17} cm^{-3} while their energy states in the bandgap (at the 0.57 eV and 0.29 eV below and above the conduction band and valence band edges, respectively) were constant [18]. However, the defect density of shallow defects that are the single donor and single acceptor were kept at 3×10^{11} cm^{-3}, and 3×10^{10} cm^{-3} respectively [23], all the time. The 3D-MAPI has shown low shallow defect density, which has not shown a considerable effect to reduce the performance of the material. The effect of the deep defect densities on the SRH recombination, which mainly causes to control the performance of the 3D-MAPI, was only investigated by considering different deep defect densities in the 3D-MAPI. In this study, the influence of the deep defect on the cell performance can be studied by using the dark saturation current density curves for different defect densities since dark saturation current density is used as a measure of the recombination in the solar cell [24].

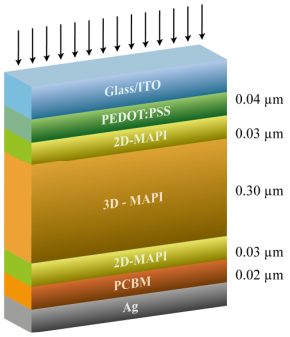

Fig. 1. The device structure of the 2D/3D/2D baseline solar cell model.

The one-dimensional Solar Cell Capacitance Simulator (SCAPS-1D) software has been used to numerically simulate the solar cell models [25]. The Poisson equation, Continuity equations for electron and holes, and carrier transport equation have been used in the program of the SCAPS-1D software [26]. In this study, we have modeled this solar cell as a thin-film solar cell with five semiconductor layers since SCAPS-1D has been developed for solar cell models that should contain equal or less than seven semiconductor layers in the cell model that should be a thin-film solar cell [27]. The perovskite cell model was simulated by changing the deep defect density in the 3D-MAPI layer. The effect of Shockley-Read-Hall (SRH) recombination was mainly considered in this solar cell simulation study since Radiative and Auger recombination do not change with deep defect density. The J-V characteristics, open-circuit voltages, Fill Factors, EQE

curves, and power conversion efficiencies of perovskite solar cells were numerically obtained under AM1.5G Sun spectrum illumination (1000 W/m^2) and ambient temperature (300 K) using SCAPS-1D.

TABLE I. SIMULATION PARAMETERS USED IN THE PEROVSKITE CELL MODEL

Parameters	Layers of the solar cell model				
	PEDOT:PSS	*2D-MAPI*[a]	*3D-MAPI*[b]	*2D-MAPI*[a]	*PCBM*
Thickness (nm)	40	30	300	30	20
Bandgap (eV)	1.55 [16]	1.63 [19]	1.55 [17]	1.63 [19]	2.0 [16]
Electron Affinity (eV)	3.63 [16]	3.9	3.9 [17]	3.9	4.3 [16]
Relative Permittivity	3.0 [16]	6.5	6.5 [17]	6.5	4.0 [16]
Effective conduction band density (cm^{-3})	1×10^{19} [16]	1.94×10^{20}	2.8×10^{18} [16]	1.94×10^{20}	1×10^{19} [16]
Effective valence band density (cm^{-3})	1×10^{19} [16]	1.94×10^{20}	3.9×10^{18} [16]	1.94×10^{20}	1×10^{19} [16]
Electron mobility (cm^2/V.c)	9×10^{-3} [16]	414 [19]	24	414 [19]	1×10^{-2} [16]
Hole mobility (cm^2/V.c)	9×10^{-3} [16]	1187 [19]	24	1187 [19]	1×10^{-2} [16]
Donor concentration (cm^{-3})	0 [16]	1×10^{16}	1×10^{16} [16]	1×10^{16}	5×10^{17} [16]
Acceptor concentration (cm^{-3})	3×10^{17} [16]	1×10^{16}	1×10^{16} [16]	1×10^{16}	0 [16]

[a] Two-dimensional sheets of Methylammonium lead iodide ($CH_3NH_3PbI_3$), DFT.
[b] Methylammonium lead iodide ($CH_3NH_3PbI_3$).

III. RESULTS/OBSERVATIONS

Fig. 2 represents the semi-logarithmic dark saturation current density vs voltage curves for different deep defect densities. The dark saturation current density of the solar cell has increased with the deep defect density in the 3D-MAPI. According to the plot, dark saturation current density can be decreased by reducing deep defect density. Also, low dark saturation current density causes to show higher light current density and higher open-circuit voltage in the solar cell. Dark saturation current is a measure of the recombination in the solar cell [24]. The large dark saturation current indicates large recombination in the solar cell.

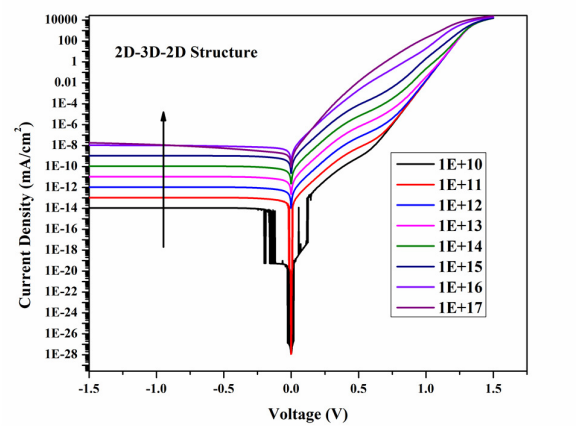

Fig. 2. Semi logarithmic dark saturation current density vs voltage curves for different deep defect densities in the 3D-MAPI layer of the 2D/3D/2D cell model.

Fig. 3 illustrates the SRH recombination current density vs voltage curve. According to the curve, the SRH recombination current density has significantly increased after the deep defect density of 10^{12} cm^{-3}. The increment of the deep defect density, in the 3D-MAPI layer, has increased the SRH recombination in the solar cell, due to the increment of the dark saturation current as shown in Fig. 2. According to these results, deep defect density should be reduced from 10^{12} cm^{-3} to as much as it can be reduced. Also, it shows that deep defect density should not exceed 10^{12} cm^{-3} to minimize the SRH recombination in the 3D-MAPI absorber layer.

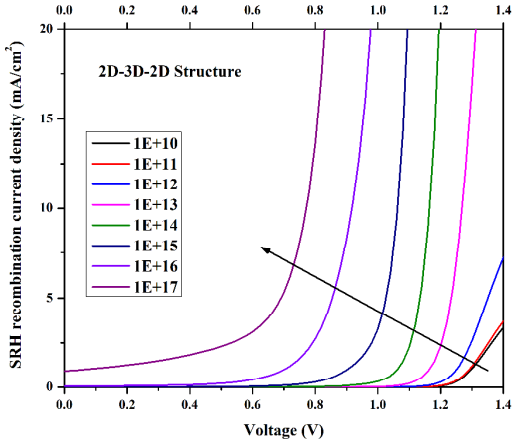

Fig. 3. SRH recombination current density variation with different deep defect densities in the 3D-MAPI layer of the 2D/3D/2D cell model.

The current density (J) vs voltage (V) curve for different deep defect densities in the 3D-MAPI layer is shown in Fig. 4. According to Fig. 4, the open-circuit voltage of the cell model has significantly changed with deep defect density in the 3D-MAPI layer. The open-circuit voltage has increased when the deep defect density was decreased in the simulation study. According to these curves, the open-circuit voltage has not shown a considerable change in the deep defect density range of 10^{10}-10^{13} cm^{-3}, in which the cell model has shown maximum fill factor [15] due to the maximum area above the J-V curve. Also, deep defect density should not exceed 10^{13} cm^{-3} to get the higher open-circuit voltage. The current density of the solar cell has not shown considerable change with the different deep defect densities.

Fig. 5 illustrates the External Quantum efficiency (EQE) vs wavelength curve of the cell model. According to the EQE curve, the solar cell has shown high performance in the wavelength range of 300-800 nm as shown in Fig. 5. The solar cell model has shown the best performance in the wavelength range of 300-450 nm, due to the high light absorption of the 3D-MAPI layer in that range. The EQE curve has represented a decrement after wavelength of about 450 nm since the light absorption in the 3D-MAPI has reduced after 450 nm [21].

However, the 3D-MAPI absorber can give External Quantum Efficiency (EQE) up to 800 nm since the bandgap of 3D-MAPI is 1.55 eV that is relevant to about 800 nm.

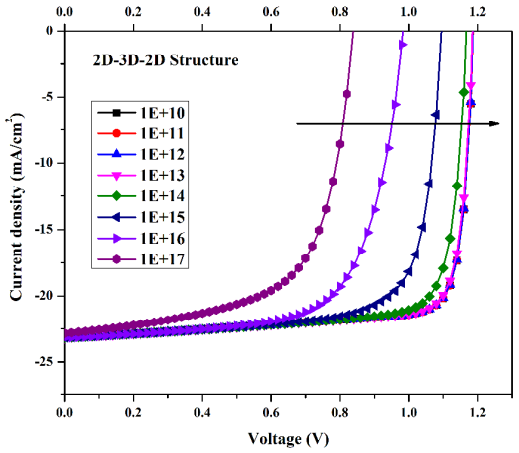

Fig. 4. Current density variation with different deep defect densities in the 3D-MAPI layer of the 2D/3D/2D perovskite cell model.

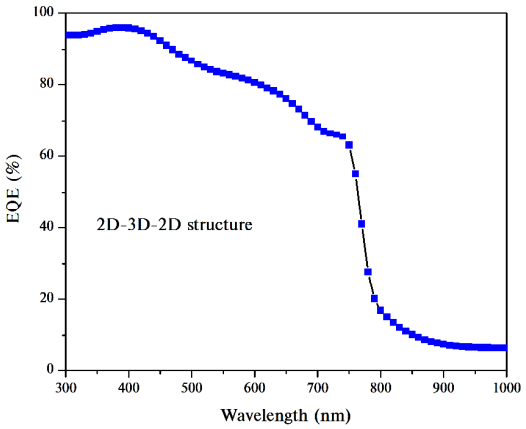

Fig. 5. Quantum efficiency vs wavelength curve of the 2D/3D/2D solar cell model.

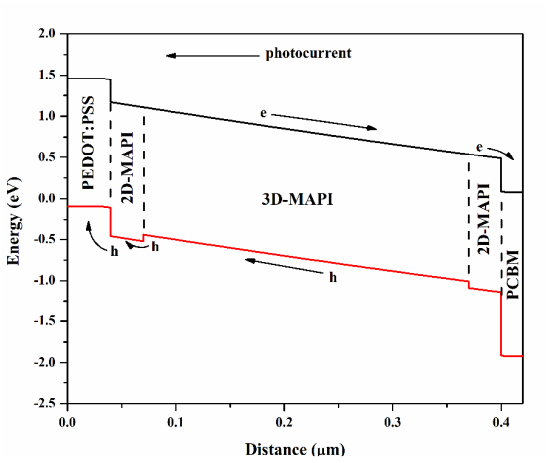

Fig. 6. The energy band diagram of the solar cell model at thermal equilibrium.

The energy band diagram of the solar cell model is illustrated in Fig. 6. According to the energy band diagram, the generated electrons in the conduction band can easily move to the back contact. At the same time, holes cannot easily move to the hole transporting layer (PEDOT:PSS) due to the small energy spike of the 2D-MAPI layer that is located in between the PEDOT:PSS layer and 3D-MAPI absorber layer, towards PEDOT:PSS. Due to that reason, generated holes have to move by overcoming the energy barrier of the 2D-MAPI layer. The power conversion efficiency of the solar cell model can be also increased by aligning the valence band of the cell model, which can be done by tuning the bandgap of 3D-MAPI. Moreover, the cell performance can be enhanced by applying band bending to the 2D-MAPI layer at PEDOT:PSS/2D-MAPI interface in the cell model.

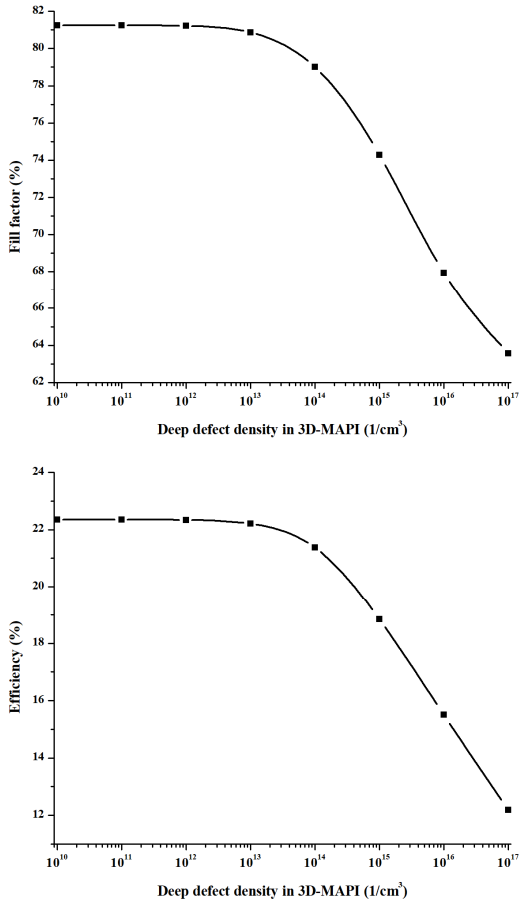

Fig. 7. Fill factor and efficiency variation with different deep defect densities in the 3D-MAPI layer of the 2D/3D/2D cell model.

According to Fig. 7, the Fill factor has reduced when the deep defect density was increased in the cell model. The reduction of the Fill factor has started when the deep defect density exceeds 10^{12} cm^{-3}. Also, the efficiency vs defect density graph shows the considerable decrement of the efficiency in the deep defect density range of 10^{12}-10^{17} cm^{-3}. According to these results, deep defect density should not exceed 10^{12} cm^{-3} in the 3D-MAPI layer to get higher efficiency of the solar cell.

IV. Conclusions

It is been observed that the deep defect density in the 3D-MAPI layer can control the perovskite solar cell performance. When the deep defect density range is varied from 10^{10}-10^{12} cm^{-3} the solar cell has shown high performance. This is also confirmed by the dark saturation current, which depends on the deep defect density. The dark saturation current should be minimized to increase the performance of the solar cell. The reduction of the deep defect density (from 10^{17} to 10^{12} cm^{-3}) causes to increase in the open-circuit voltage of the solar cell models, which showed an increment of the open-circuit voltage of about 42%. According to that, the power conversion efficiency of the solar cells can be enhanced by about 83% reducing the deep defect density in the 3D-MAPI layer of the solar cell from 10^{17} to 10^{12} cm^{-3}. However, by considering SRH recombination in the solar cells, deep defect density should not exceed 10^{12} cm^{-3}. The formation of the deep defects that are located in the bandgap of the 3D-MAPI should be minimized in the deposition process of the perovskite solar cell. Our research findings will be helpful to design an efficient and low degraded, perovskite solar cell by optimizing deep defects in the 3D-MAPI layer.

Acknowledgment

This research work was financially supported by the research grant from the Ministry of Science, Technology and Research, Government of Sri Lanka, under the Indo-Sri Lanka bilateral agreement (Grant No. MSTR/TRD/AGR/03/02/15).

References

[1] M. K. Nazeeruddin, "Twenty-five years of low-cost solar cells," *Nature,* vol. 538, pp. 463-464, 2016.

[2] Best Research-Cell Efficiency Chart, NREL, https://www.nrel.gov/pv/cell-efficiency.html, (accessed Jan. 20, 2021).

[3] D. B. Mitzi, "Solution-processed inorganic semiconductors," *Journal of Materials Chemistry,* vol. 14, pp. 2355-2365, 2004.

[4] B. Philippe, B.-W. Park, R. Lindblad, J. Oscarsson, S. Ahmadi, E. M. Johansson*, et al.*, "Chemical and Electronic Structure Characterization of Lead Halide Perovskites and Stability Behavior under Different Exposures A Photoelectron Spectroscopy Investigation," *Chemistry of Materials,* vol. 27, pp. 1720-1731, 2015.

[5] P. Chen, Y. Bai, S. Wang, M. Lyu, J. H. Yun, and L. Wang, "In situ growth of 2D perovskite capping layer for stable and efficient perovskite solar cells," *Advanced Functional Materials,* vol. 28, p. 1706923, 2018.

[6] F. Zhang, D. H. Kim, and K. Zhu, "3D/2D multidimensional perovskites: balance of high performance and stability for perovskite solar cells," *Current Opinion in Electrochemistry,* vol. 11, pp. 105-113, 2018.

[7] M. H. Li, H. H. Yeh, Y. H. Chiang, U. S. Jeng, C. J. Su, H. W. Shiu*, et al.*, "Highly efficient 2D/3D hybrid perovskite solar cells via low-pressure vapor-assisted solution process," *Advanced Materials,* vol. 30, p. 1801401, 2018.

[8] A. Luque and S. Hegedus, *Handbook of photovoltaic science and engineering*: John Wiley & Sons, 2011.

[9] R. Brakkee and R. M. Williams, "Minimizing defect states in lead halide perovskite solar cell materials," *Applied Sciences,* vol. 10, p. 3061, 2020.

[10] E. Aydin, M. De Bastiani, and S. De Wolf, "Defect and contact passivation for perovskite solar cells," *Advanced Materials,* vol. 31, p. 1900428, 2019.

[11] N. Adihetty, M. Attygalle, N. Narayan, and P. Jha, "A study of the performance of organometal trihalide perovskite solar cell due to defects in bulk CH3NH3PbI3 (MAPI) perovskite layer," *International Journal of Multidisciplinary Studies,* vol. 8, pp. 101-112, 2021.

[12] A. Chen, K. Zhu, Q. Shao, and Z. Ji, "Understanding the effects of TCO work function on the performance of organic solar cells by numerical simulation," *Semiconductor Science and Technology,* vol. 31, p. 065025, 2016.

[13] M. Girtan and M. Rusu, "Role of ITO and PEDOT: PSS in stability/degradation of polymer: fullerene bulk heterojunctions solar cells," *Solar Energy Materials and Solar Cells,* vol. 94, pp. 446-450, 2010.

[14] S. Heo, G. Seo, K. T. Cho, Y. Lee, S. Paek, S. Kim*, et al.*, "Dimensionally engineered perovskite heterostructure for photovoltaic and optoelectronic applications," *Advanced Energy Materials,* vol. 9, p. 1902470, 2019.

[15] D. W. de Quilettes, S. M. Vorpahl, S. D. Stranks, H. Nagaoka, G. E. Eperon, M. E. Ziffer*, et al.*, "Impact of microstructure on local carrier lifetime in perovskite solar cells," *Science,* vol. 348, pp. 683-686, 2015.

[16] B. Olyaeefar, S. Ahmadi-Kandjani, and A. Asgari, "Classical modelling of grain size and boundary effects in polycrystalline perovskite solar cells," *Solar Energy Materials and Solar Cells,* vol. 180, pp. 76-82, 2018.

[17] F. Azri, A. Meftah, N. Sengouga, and A. Meftah, "Electron and hole transport layers optimization by numerical simulation of a perovskite solar cell," *Solar energy,* vol. 181, pp. 372-378, 2019.

[18] D. Meggiolaro, S. G. Motti, E. Mosconi, A. J. Barker, J. Ball, C. A. R. Perini*, et al.*, "Iodine chemistry determines the defect tolerance of lead-halide perovskites," *Energy & Environmental Science,* vol. 11, pp. 702-713, 2018.

[19] S. R. Kumavat, Y. Sonvane, D. Singh, and S. K. Gupta, "Two-dimensional ch3nh3pbi3 with high efficiency and superior carrier mobility: A theoretical study," *The Journal of Physical Chemistry C,* vol. 123, pp. 5231-5239, 2019.

[20] W. Tress, "Perovskite solar cells on the way to their radiative efficiency limit–insights into a success story of high open-circuit voltage and low recombination," *Advanced Energy Materials,* vol. 7, p. 1602358, 2017.

[21] L. J. Phillips, A. M. Rashed, R. E. Treharne, J. Kay, P. Yates, I. Z. Mitrovic*, et al.*, "Dispersion relation data for methylammonium lead triiodide perovskite deposited on a (100) silicon wafer using a two-step vapour-phase reaction process," *Data in brief,* vol. 5, pp. 926-928, 2015.

[22] M. Chowdhury, S. Shahahmadi, P. Chelvanathan, S. Tiong, N. Amin, K. Techato*, et al.*, "Effect of deep-level defect density of the absorber layer and n/i interface in perovskite solar cells by SCAPS-1D," *Results in Physics,* vol. 16, p. 102839, 2020.

[23] V. Adinolfi, M. Yuan, R. Comin, E. S. Thibau, D. Shi, M. I. Saidaminov*, et al.*, "The in-gap electronic state spectrum of methylammonium lead iodide single-crystal perovskites," *Advanced materials,* vol. 28, pp. 3406-3410, 2016.

[24] E. Meyer, "Extraction of saturation current and ideality factor from measuring Voc and Isc of photovoltaic modules," *International Journal of Photoenergy,* vol. 2017, 2017.

[25] A. Niemegeers, M. Burgelman, K. Decock, J. Verschraegen, and S. Degrave, "SCAPS manual," *University of Gent,* vol. 13, 2014.

[26] M. Mostefaoui, H. Mazari, S. Khelifi, A. Bouraiou, and R. Dabou, "Simulation of high efficiency CIGS solar cells with SCAPS-1D software," *Energy Procedia,* vol. 74, pp. 736-744, 2015.

[27] R. Wei, "Modelling of perovskite solar cells," Queensland University of Technology, 2018.